Effect of equal channel angular pressing on the microstructure and mechanical properties of Al-10Zn-2Mg alloy

G. K. Manjunath, G. V. Preetham Kumar, and K. Udaya Bhat

Citation: AIP Conference Proceedings **1943**, 020067 (2018); doi: 10.1063/1.5029643
View online: https://doi.org/10.1063/1.5029643
View Table of Contents: http://aip.scitation.org/toc/apc/1943/1
Published by the American Institute of Physics

Effect of Equal Channel Angular Pressing on the Microstructure and Mechanical properties of Al-10Zn-2Mg Alloy

G. K. Manjunath[1, a)] G. V. Preetham Kumar[1, b)] and K. Udaya Bhat[1, c)]

[1]*Department of Metallurgical and Materials Engineering, National institute of Technology Karnataka, Surathkal, Mangalore - 575025, India*

[a)]Corresponding author: manjugk2001@gmail.com
[b)]pkphd@hotmail.com
[c)]udayabhatk@gmail.com

Abstract. The current investigation is focused on evaluating the mechanical properties and the microstructure of cast Al-10Zn-2Mg alloy processed through equal channel angular pressing (ECAP). The ECAP processing was attempted at minimum possible processing temperature. Microstructural characterization was carried out in optical microscopy, scanning electron microscopy, transmission electron microscopy and X-ray diffraction analysis. Hardness measurement and tensile tests were employed to estimate the mechanical properties. Experimental results showed that, ECAP processing leads to noticeable grain refinement in the alloy. Reasonable amount of dislocations were observed in the ECAP processed material. After ECAP processing, precipitates nucleation in the material was detected in the XRD analysis. ECAP leads to considerable enhancement in the mechanical properties of the material. After ECAP processing, microhardness of the material is increased from 144 Hv to 216 Hv. Also, after ECAP processing the UTS of the material is increased from 140 MPa to 302 MPa. The increase in the mechanical properties of the alloy after ECAP processing is due to the dislocation strengthening and grain refinement strengthening. Finally, fracture surface morphology of the tensile test samples also studied.

Keywords: Mechanical properties; Al-Zn-Mg alloy; ECAP; Microstructure.

INTRODUCTION

Development of the ultrafine grained (UFG) materials through severe plastic deformation (SPD) is an auspicious procedure to enhance the mechanical properties of metals and alloys for structural applications [1]. Amongst, all SPD methods, ECAP is a trustworthy technique to develop UFG materials in metals [2]. In ECAP process, material is subjected to simple shear deformation without any considerable change in the cross-sectional dimension of the material [3]. Aluminium and its alloys are widely adopted in structural, industrial and transport applications due to their low density, high strength and outstanding corrosion resistance characteristics. In the present day, heat treatable Al–Zn–Mg alloys have gained abundant interest as the main materials in aerospace and aviation applications as well as marine and automotive industries [4].

Several investigations have been stated to study the outcome of ECAP processing predominantly on mechanical properties of the materials. Horita et al. reported the effect of the sample size on the mechanical properties and the microstructure of the Al 7075 alloy processed by ECAP and load required for ECAP processing was also examined. It was reported that, strength of the material increased with ECAP processing. It also reported that, maximum load required for the ECAP processing is calculated by the sample strength and not by sample dimensions [5]. Shaeri et al. studied the effect of the ECAP processing temperature on the mechanical properties and the microstructure of Al-Zn-Mg-Cu alloy. It was reported that, with increase in the processing temperature leads to an increase in the grain size and the fraction of low angle grain boundaries. Also, dislocation density decreases significantly. It also reported that, material processed at temperature range from room temperature to 120 ºC shows the maximum mechanical properties than the material processed at temperature range from 120 ºC to 180 ºC [6]. In this regard, the material being considered in the present study was attempted to process at minimum possible processing temperature.

EXPERIMENTS

TABLE 1. Composition the alloy found in optical emission spectroscopy

Element	Al	Zn	Mg	Fe	Si	Mn	Cu	Zr	Ni	Ti	Pb	Cr
Weight %	87.3	10.1	2.1	0.23	0.16	0.074	0.022	0.005	0.002	0.003	0.002	0.002

The material used in the present investigation was prepared by gravity die casting process with appropriate quantity of commercial pure aluminium, high purity zinc and high purity magnesium. After casting, composition of the material was verified in optical emission spectroscopy (OES). Table 1 indicates the composition of the material verified through OES. After casting, homogenization treatment of the material was carried out for a time span of 20 hours at 480 ºC. Features of the ECAP die adopted in the present investigation are presented in Table 2. The literature on the ECAP indicates that the strength could be maximized by processing the material at low temperature. In this regard, material was attempted to process at minimum possible temperature. Molybdenum disulphide (MoS_2) lubricant was applied on the sample and in the cylindrical channel of the die to avoid the friction. The ECAP processing experiments were conducted in a 40 ton universal testing machine at a pressing speed ≈ 0.5 mm per second. The ECAP die was fabricated from hot die steel (HDS) and heat treated to 50 HRc. ECAP die was manufactured in split type design and clamped with the help of bolts and nuts.

TABLE 2. Features of the ECAP die

Diameter of the channel	Angle of the die (Φ)	Outer arc of curvature (Ψ)	Strain in each pass
16 mm	120º	30º	0.667

For microstructural study, samples were sectioned into discs in transverse direction followed by polishing with abrasive papers and cloth polishing to mirror finish (Cloth polishing was carried out in aluminium oxide powder mixed in water). Finally, the samples were etched in Keller's etchant. Micrographs of the material were captured using optical microscopy (OM), scanning electron microscopy (SEM) and transmission electron microscopy (TEM). For TEM analysis, samples were prepared by thinning followed by dimpling and ion milling. Grain size measurements were carried out by linear interception method. To identify the phases present in the material X-ray diffraction (XRD) analysis was conducted. To evaluate the mechanical properties of the material, hardness measurement and tensile tests were conducted. To check the repeatability of the results, 10 hardness measurements were carried out and average values were considered. Similarly, to check the repeatability of the results in tensile testing 3 specimens were tested and average values were considered. After tensile testing fracture surface morphology of the tensile test samples were also studied in SEM.

RESULTS AND DISCUSSION

(a) (b) (c)

FIGURE 1. Al-10Zn-2Mg alloy ECAP processed at (a) room temperature, (b) 100 ºC and (c) 125 ºC

(a) (b)

FIGURE 2. Al-10Zn-2Mg alloy ECAP processed at 150 ºC (a) 1 pass and (b) 2 pass

Figure 1 shows the macroviews of the samples which were failed during ECAP processing at room temperature, 100 ºC and 125 ºC, in the first pass itself. The material was successfully processed at 150 ºC upto one pass and samples were failed during second pass in route B_C at 150 ºC as shown in Fig. 2. It may be noted that the intensity of the crack reduces with increase in the processing temperature. Since the sample was failed during second pass, discussion and analysis of the results were concluded to first ECAP pass.

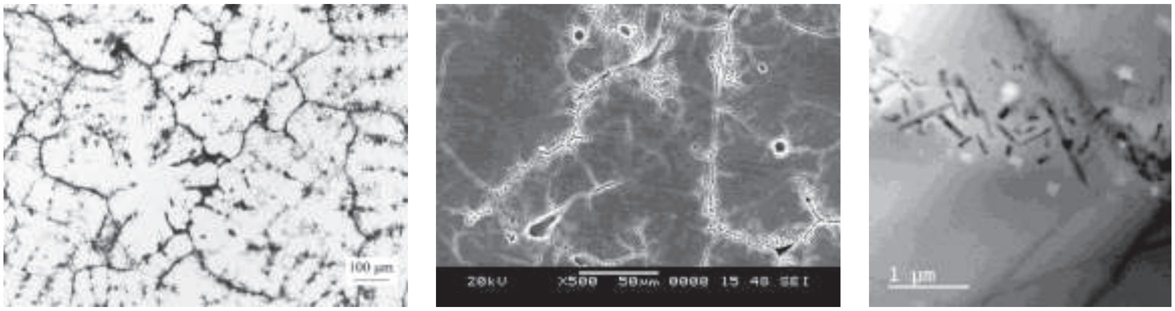

(a) (b) (c)

FIGURE 3. (a) OM micrograph, (b) SEM micrograph and (c) TEM micrographs of the alloy in cast condition

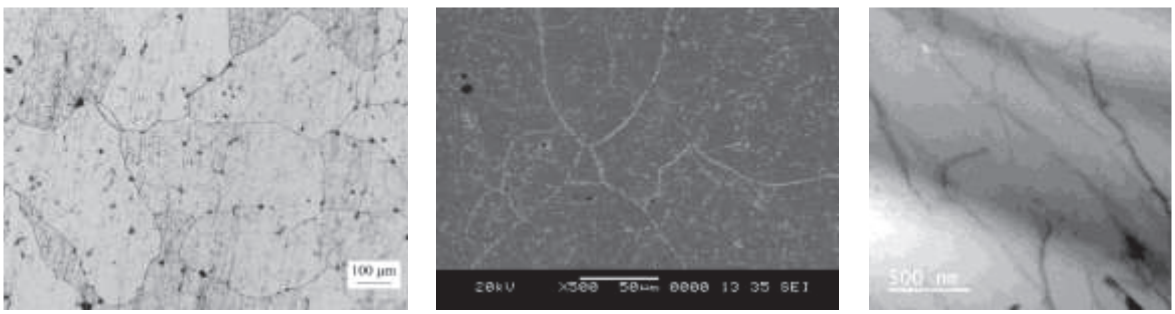

(a) (b) (c)

FIGURE 4. (a) OM micrograph, (b) SEM micrograph and (c) TEM micrographs of the alloy in homogenized condition

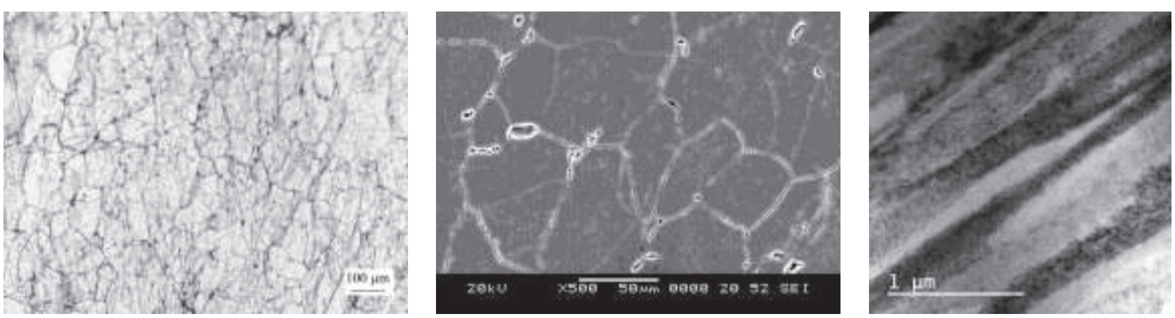

(a) (b) (c)

FIGURE 5. (a) OM micrograph, (b) SEM micrograph and (c) TEM micrographs of the alloy after one pass

Figure 3 presents the micrographs of the material in cast condition; the microstructure was constructed with dendritic structure with size 280 ± 40 µm and secondary particles (precipitates) were located in the inter-dendritic regions. These secondary particles were identified as $MgZn_2$ precipitates [7]. In Fig. 3c the morphology of the precipitates can be observed. In this condition, large rod shaped precipitates were observed. The length of the precipitates ranges from 250 nm to 750 nm. The width of the precipitates ranges from 50 nm to 100 nm. Figure 4 presents the micrographs of the material in the homogenized condition; secondary particles located in the inter-dendritic regions were uniformly dissolved in the aluminium matrix and grains boundaries were formed in the size of 260 ± 20 µm. Figure 5 presents the micrographs of the material after ECAP processing. It may be noted that, significant refinement in the grain size was observed and sub-grain boundaries were formed inside the grains. Also, precipitates were developed near the grain boundaries. A grain size of 60 ± 10 μm was perceived. From TEM observations, it is revealed that in the ECAP processed sample, the presence of elongated grains and reasonable amount of dislocations were observed as shown in Fig. 5c.

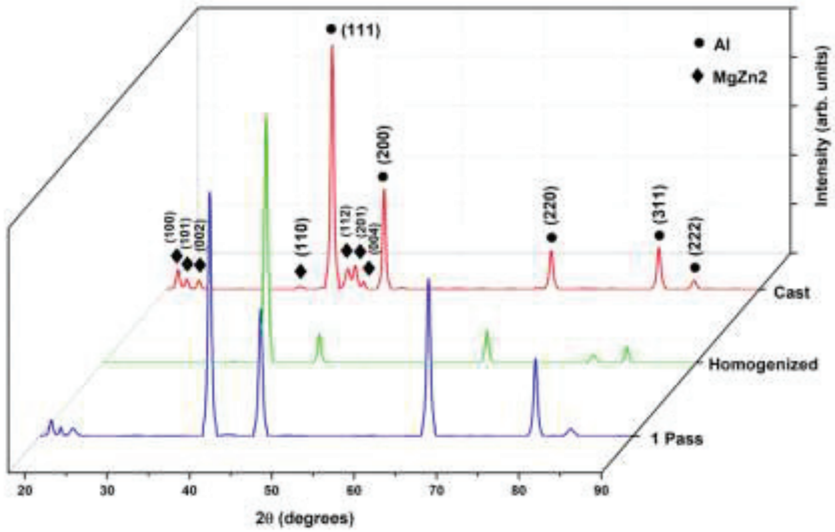

FIGURE 6. XRD plots of the alloy in various conditions

Figure 6 illustrates the XRD plots of the cast, homogenized and one ECAP pass samples. In cast sample, relatively high intensity peaks for aluminium was observed. Also, some small intensity peaks near 20º and 45º were also observed. Peaks near 20º relate to Guinier-Preston (GP) zones and peaks near 45º relate to $MgZn_2$ secondary phase [8]. In the homogenized material, peaks related to only aluminium was observed. Because after the homogenization treatment, precipitates located in the inter-dendritic regions were homogeneously dispersed in the aluminium. This is in consistent with the microstructural observations on the homogenized material. After ECAP processing, along with aluminium peaks other peaks related to precipitates was observed, since the dislocations which are evolved during ECAP processing provides space for the development of the precipitates. This is in consistent with the microstructural observations on the one ECAP pass material.

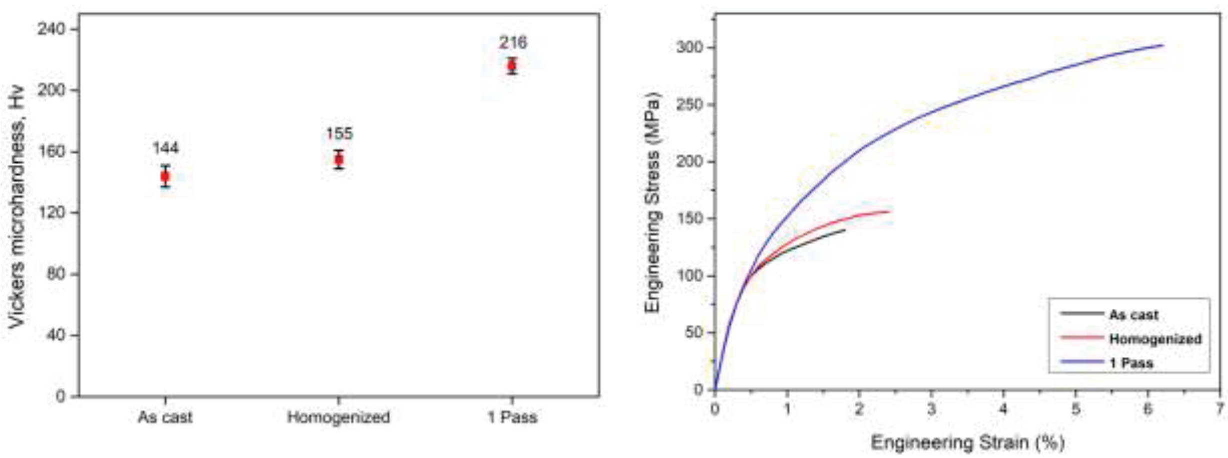

(a) (b)

FIGURE 7. (a) Microhardness (b) Engineering stress – strain curves of the alloy in various conditions

Figure 7a presents the variation of the microhardness of the material in various conditions. The microhardness of the material in the cast condition is 144 ± 7 Hv and after homogenization treatment the microhardness of the material is enhanced to 155 ± 6 Hv. After one ECAP pass, the microhardness of the material is enhanced to 216 ± 5 Hv (50% increase from the cast material). It was perceived that, processing by ECAP leads to significant enhancement in the microhardness of the material. Kim et al reported that, after one ECAP pass, large improvement in the microhardness was observed compared to later passes [9]. Similar behavior was also observed in Al 7010 alloy subjected to ECAP upto one pass [10]. Hence it can be concluded that, ECAP processing upto one number of pass will also provide beneficial outcomes. The enhancement in the microhardness of the material is credited to the reduction in the grain size of the material and strain hardening during ECAP processing [11].

TABLE 3. Mechanical properties of the alloy in various conditions

Condition of the alloy	Microhardness (Hv)	Yield strength (MPa)	Ultimate tensile strength (MPa)	% Elongation to failure
Cast	144 ± 7	96 ± 10	140 ± 10	1.8 ± 0.4
Homogenized	155 ± 6	112 ± 10	156 ± 10	2.4 ± 0.4
1 Pass	216 ± 5	217 ± 8	302 ± 8	6 ± 0.3

Figure 7b presents the engineering stress – strain curves of the alloy in various conditions. Table 3 presents the mechanical properties of the alloy in various conditions. The yield stress (YS) was estimated by projecting an offset line parallel to the slope of the stress-strain curve with 0.2% offset. Crossing point of the stress–strain curve and offset line will be considered as the YS value at 0.2% strain. YS of the alloy in the cast condition is 96 ± 10 MPa and after homogenization treatment the YS of the alloy is enhanced to 112 ± 10 MPa. After one pass, the YS of the alloy is enhanced to 217 ± 8 MPa. It was perceived that, processing by ECAP leads to a considerable enhancement in the YS of the alloy. Ultimate tensile strength (UTS) of the alloy in the cast condition is 140 ± 10 MPa and after homogenization treatment the UTS of the alloy is enhanced to 156 ± 10 MPa. After one pass, the UTS of the alloy is enhanced to 302 ± 8 MPa (116% increase from the cast material). Similar to YS, the UTS of the alloy enhanced with ECAP processing. Enhancement in the strength of the alloy after ECAP processing is due to the dislocation strengthening and Hall-Petch effect [12]. In the cast material, owing to the existence of micro-porosity and the dendritic structure, elongation to failure of the alloy was perceived to be very less (around 1.8 ± 0.4). After the homogenization treatment, marginal improvement in the elongation to failure was perceived (about 2.4 ± 0.4). On the contrast, processing by ECAP leads to an enhancement in the elongation to failure of the alloy. After one pass, the elongation to failure of the alloy was enhanced to 6 ± 0.4. The increase in ductility of the material after ECAP processing is due to the refined microstructure.

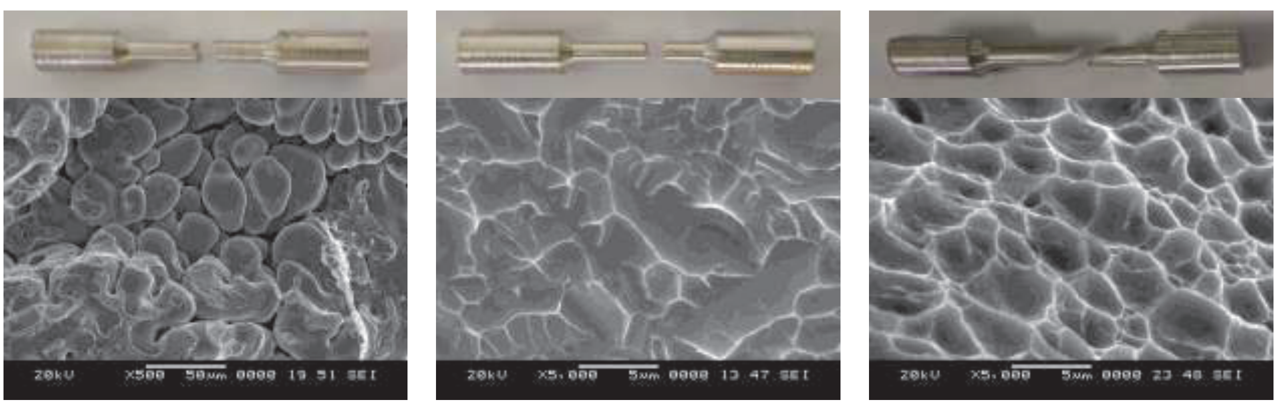

(a) (b) (c)

FIGURE 8. Tensile test samples and SEM micrographs of the fracture surfaces after tensile testing (a) cast, (b) homogenized and (c) 1 pass

Figure 8 presents the tensile test samples and SEM micrographs of the fracture surfaces after tensile testing of the material in different conditions. It was witnessed that, failure in the cast material happened perpendicular to the axis of the tensile specimen. The fracture mode witnessed in the cast material is brittle fracture. Also, the fracture surface of the cast sample was compiled with dendrites of size 25 μm and micro-porosities as shown in Fig 8a. Similar to cast material, failure in the homogenized material happened perpendicular to the axis of the tensile specimen. The fracture mode witnessed in the homogenized sample is brittle fracture. But, the fracture surface was compiled with large size dimples of size 5 μm. After one ECAP pass, failure of the material happened nearly 45º to the axis of the tensile specimen. The fracture mode witnessed in the ECAP processed materials is shear fracture. Size of the dimple is decreased to 2.5 μm and showed a homogeneous spreading through the fracture surfaces. Similar behavior was also witnessed in Al-40Zn alloy subjected to ECAP [12]. The decrease in the size of the dimples is due grain refinement during ECAP processing.

CONCLUSIONS

In the current investigation, cast Al-10Zn-2Mg alloy was attempted to ECAP processing at minimum possible temperature in 120º die. The material was successfully processed upto one number of pass at 150 ºC. Significant refinement in the grain size was observed after ECAP processing and considerable amount of dislocations were developed in the material. After ECAP, nucleation of the precipitates was observed in the material. Also, ECAP led to significant enhancement in the strength and the hardness of the alloy. After ECAP, 50% increase in the hardness and 116% increase in the UTS of the alloy was observed from the cast condition. Finally, it can be concluded that, ECAP processing upto one number of pass will also provide valuable outcomes. Dendritic structure was witnessed in the fracture surface of the cast material tensile specimen. Whereas, dimples were witnessed in the fracture surface of the ECAP processed material tensile specimen.

REFERENCES

1. R.Z. Valiev, R.K. Islamgaliev and I.V. Alexandrov, Prog. Mater. Sci. **45**, 103-189 (2000).
2. R. Z. Valiev and T. G. Langdon, Prog. Mater. Sci. **51**, 881–981 (2006).
3. M.J. Zehetbauer and Y.T. Zhu, *Bulk Nanostrucutred Materials* (Wiley-VCH Weinheim 2009) pp. 203-215.
4. M.H. Shaeri, M.T. Salehi, S.H. Seyyedein, M.R. Abutalebi and J.K. Park, Mater. Des. **57**, 250-257 (2014).
5. Z. Horita, T. Fujinami, M. Nemoto and T.G. Langdon, J. Mater. Process. Technol. **117**, 288-292 (2001).
6. M.H. Shaeri, M. Shaeri, M. Ebrahimi, M.T. Salehi and S.H. Seyyedein, Prog. Nat. Sci. Mater. Int. **26**, 182-191 (2016).
7. S. Zhang, W. Hu, R. Berghammer and G. Gottstein, Acta Mater. **58**, 6695-6705 (2010).
8. Y.H. Zhao, X.Z. Liao, Z. Jin, R.Z. Valiev and Y.T. Zhu, Acta Mater. **52**, 4589-4599 (2004).
9. W.J. Kim, J.K. Kim, H.K. Kim, J.W. Park and Y.H. Jeong, J. Alloys Compd. **450**, 222-228 (2008).
10. E.A. El-Danaf, Mater. Des. **32**, 3838-3853 (2011).
11. L.J. Zheng, H.X. Li, M.F. Hashmi, C.Q. Chen, Y. Zhang and M.G. Zeng, J. Mater. Process. Technol. **171**, 100-107 (2006).
12. O. Saray and G. Purcek, J. Mater. Process. Technol. **209**, 2488-2498 (2009).